Quasi-quantitative combined small signal analysis to predict radiated emission of DC-DC buck converters

Gergely Friedl, Miklós Kuczmann

Abstract: This paper proposes a quasi-quantitative combined small signal simulation approach to predict low frequency radiated emission of DC-DC buck converters. A simulation methodology to efficiently replace transient analysis with small signal analysis, and the environmental effects on the low frequency radiated emission are discussed. The efficiency and accuracy of the approach is presented through measurements and simulations performed on an evaluation board designed for the TPS54560 type switching IC. The simulation results fit very well to the measured radiated emission performance of the DC-DC converter module. With the proposed approach, fast and accurate parametric results can be achieved without using time consuming transient analysis.

Keywords: electromagnetic compatibility, simulation, radiated emission, DC-DC converter

I. Introduction

In order to reduce power dissipation of different electronic devices built into vehicles, switched-mode power supplies are frequently used for voltage conversion in the automotive industry due to their high efficiency compared to other voltage regulation techniques. One of the most painful drawbacks of using switched-mode voltage converters is their electromagnetic interference (EMI) performance. Even a low power DC-DC converter can be the main reason for failing automotive radiated emission tests, which is necessary to comply with international regulations. The automotive industry demands high quality and low cost devices, but designing a low cost low EMI converter is still a challenging task for electromagnetic compatibility (EMC) and simulation engineers. The main source of radiated emission of DC-DC (where DC stands for direct current) converters in the frequency range 0.1 – 30 MHz is due to the switching operation of the high side and low side active components. The simulation engineer can choose from many methods to predict the EMI in the monopole range, from the fastest and most simplistic but less accurate capacitive coupling models (e.g. in [1], [2], [28] and [29]) to the time consuming but more accurate full wave 3 dimensional (3D) simulation combined with transient circuit analysis (e.g. in [3],[4] and [27]). All the methodologies have their advantages and disadvantages, the proposed approach aims to provide fast and accurate results at the same time.

Semi-anechoic chambers can be easily modelled at frequencies, where the pyramid absorbers combined with ferrite tiles can be considered as a nonreflective surface. Since it is only valid above ~100 MHz [5], modelling a semi-anechoic chamber in the frequency range of interest is[1] quite challenging. Many aspects of chamber modelling have been analyzed and taken into account in order to achieve quasi-quantitative results.

II. DC-DC buck converters

While the battery of a vehicle provides voltage around 13 Volts, microcontrollers and integrated circuits demand lower voltage levels, e.g. 3.3 or 5 Volts. The usage of linear voltage regulators is usually not acceptable due to the high dissipated power, thus making the efficient DC-DC buck converters indispensable parts for many automotive electronic devices.

The continuous operation of buck converters can be separated into two operation states (see in Fig. 1.) [6][7]:

- On state: Switching metal-oxide-semiconductor field-effect transistor (MOSFET) conducting, the discharging input buffer capacitors provide current for the output stage, meanwhile the output inductor accumulates energy.
- Off state: The inductor discharges the accumulated energy, thereby the diode switches to freewheeling state.

The resulting output voltage can be easily calculated as

$$V_{out} = V_{in} \cdot T_{ON}/(T_{OFF} + T_{ON}), \quad (1)$$

where V_{out} and V_{in} is the output and input voltage of the DC-DC converter module, and T_{ON} and T_{OFF} are the time spent by the converter in ON and OFF state respectively.

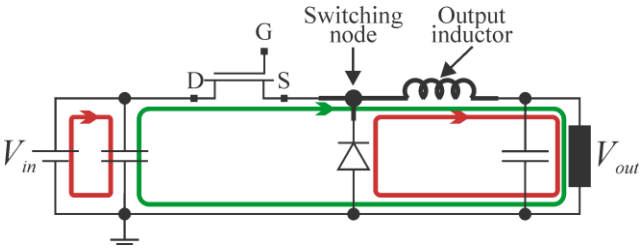

Fig. 1. DC-DC converter operation states.

III. RADIATED EMISSION OF DC-DC CONVERTERS

During EMC development of buck converters, the most

Received: 18.05.2023
Published: 10.06.2023

https://doi.org/10.47978/TUS.2023.73.01.001

G. Friedl is with Széchenyi István University, Győr, Hungary (friedl.gergely@gmail.com)
M. Kuczmann is with Széchenyi István University, Department of Power Electronics, and Electric Drives, Győr, Hungary (kuczmann@sze.hu)

important design parameters are the input and output filters, any aspects of the switching loop and switching node, and the switching waveform characteristics [8]. Radiated EMI behavior at frequencies, where the measuring distance is in the sub-wavelength range is usually due to capacitive and inductive couplings.

While the voltages at the input and output nets are relatively stable if the input and outfit filtering components are properly designed, the potential of the so-called switching node (highlighted in Fig. 1.) is continuously varying. During ON state, the voltage on the switching node is approximately around the battery voltage, while during OFF state it drops below ground potential by the forward voltage of the freewheeling diode. Electromagnetic radiation of buck converters (typically up to 30 MHz) is mostly related to the switching node and the output inductor. These components contribute the most to the capacitive coupling between the DC-DC converter and the monopole antenna. There are different ways to decrease the amount of coupled energy:

- Electric shielding around the entire device,
- Usage of electrically shielded output inductor,
- Decreasing the size of the switching node,
- Symmetric layout and filter design.

All of these have their advantages and disadvantages, it is up to the EMC designer, how to implement these techniques to achieve an optimally silent design.

Above 30 MHz, the main sources of the emission peaks are the common mode resonances of the test setup, the switching loop ringing and other printed circuit board (PCB) resonances [9][10]. This frequency range is out of the scope of the paper.

IV. Simulation concept

A. Outlook

During the preparation of the EMC concept of any device, it is important to reveal all the potential noise sources along with the affected frequency bands. As the complexity of the PCBs may be very high, there is an increasing demand for field simulation to support EMC development. In many cases, the goal of simulation support of EMC development is to predict, if an actual design is able to pass the validation tests. Due to the increasing complexity of devices, it is still a great challenge for simulation engineer to achieve quantitative simulation results. The main noise generating mechanisms are [11]:

- Switching events (communication signals, motor controls, DC-DC converters),
- Discharging (brush motors),
- Resonances (any device).

Resonances can be easily analyzed by appropriate electromagnetic simulations, while taking into account switching and discharging sophisticated models are necessary. In DC-DC buck converters, there are at least two high power switching devices. These are usually referred as high-side and low-side switches, which are operating as complementary switches.

The conventional and most straightforward way to analyze DC-DC converter emission is the steady state transient analysis combined with 3D simulations. To achieve accurate results, the following shall be ensured by:

- Proper component models,
- Sufficient 3D model with accurate material properties,
- Proper simulation settings, especially focusing on dynamic range and DC behavior.

For passive components, it is easy to find accurate S-parameter models. For active components the situation is a bit different. The available functional simulation (so-called SPICE) models are well suited for functional analysis, however from EMC analysis point of view, different aspects of the operation are important. As an example, switching waveforms with losses are accurately represented for lower frequencies, while the parasitic inductive and capacitive behavior is not well taken into account.

B. Quantitative small signal analysis

The proposed approach is a modified version of the recently published method (two-step combined small-signal analysis [12]) suited for lower frequency analysis. The original procedure is a sufficient tool to support the EMC development of a DC-DC converter, since it

- Provides results quickly,
- Enables parametric analysis,
- Provides reasonably accurate results.

It can be applied for EM simulations with the following limitations:

- There may be no relevant nonlinear effects,
- Qualitative investigation is sufficient for the scope of analysis,
- The changes to apply on the model exclude the ones, that take effect on the operation point.

The reason for the limitation concerning the accuracy is due to the switching loop ringing depending on the operation point and duty cycle. This ringing is caused by the discharging inductances around the switching loop. It is not possible to capture this transient behavior by small signal analysis, since the discharge is dependent on the operation point [13][14].

The basic concept is similar to the measurement based time-harmonic analysis in [15],[16] and [17]. The main idea behind the method is to ensure the possibility of parametrization by exciting artificially created resonances. To do so, the switching loop related effects shall be separated from other events, since the ringing is generated by the resonance of the switching loop, and the magnitude depends on the operation point and duty cycle. The first step is to determine the duty cycle, the switching frequency (f_{SW}), and the rise (τ_r) and fall time (τ_f) of the switching waveform. By getting rid of the ringing, the switching waveform is a simple trapezoidal signal, that does not depend on the switching loop itself. (see in Fig. 2.). By knowing the operation point of the converter, it is easy to determine the switching frequency and the duty cycle (the first is usually set by a simple resistor, the latter is calculated by (1)). Rise and fall times are safer to be measured, however, the break point in the spectra due to the rise and fall times are usually higher than 30 MHz [8]. Apart from the ringing, a switching waveform (follow in Fig. 2.) can be specified by the

following parameters:

- Switching frequency (f_{SW}), or
- Length of one period ($T = 1/f_{SW}$)
- Magnitude (A)
- Duty cycle defined as T_{ON}/T
- Rise and fall time (τ_r and τ_f)

The envelope of the spectrum of a trapezoid signal can be easily approximated as illustrated in Fig. 3.

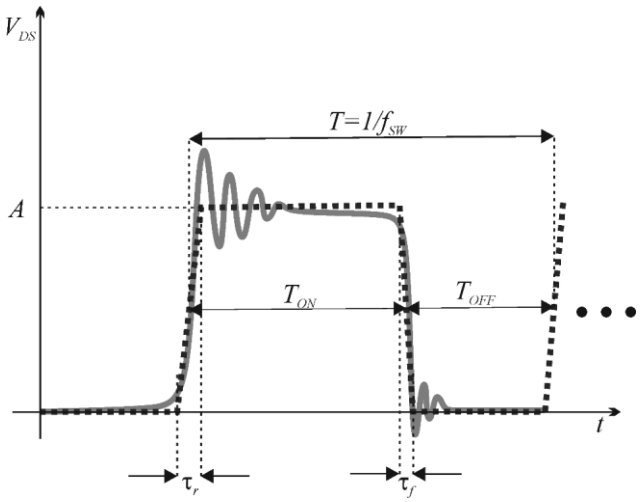

Fig. 2. Trapezoid approximation of a switching signal.

The spectrum can be easily calculated according to the *Fourier*-series expansion of the trapezoid signal [18]:

$$f(t) = \frac{AT_{ON}}{T} + \frac{2AT_{ON}}{T}\sum_{n=1}^{\infty}\left[\frac{\sin(n\pi f_{SW}T_{ON})}{n\pi f_{SW}T_{ON}}\right]\left[\frac{\sin(n\pi f_{SW}\tau_r)}{n\pi f_{SW}\tau_r}\right] \cdot \mathrm{e}^{-jn\pi f_{SW}T_{ON}}\mathrm{e}^{j2n\pi f_{SW}t}. \quad (2)$$

In Fig. 3. , the slope of the spectrum is illustrated as:

- Piecewise approximation with red color.
- Accurate envelope with blue color.
- The actual harmonic content with green color.

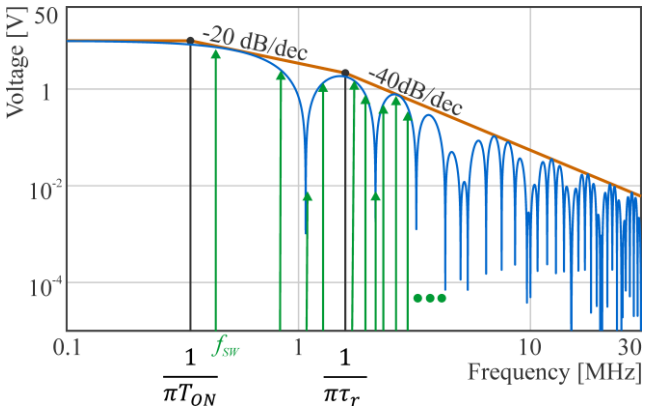

Fig. 3. Spectrum of a trapezoid signal.

Separate simulations shall be performed for every single switching state taken into account, since the overall spectrum is a combination of the spectrum of separate switching operations. The reason for that lies in the EMC measurement process. The electromagnetic emission of any device is measured with either with receiver mode or Fast-*Fourier* Transform (FFT) mode. Both observes the electromagnetic field for a sufficient amount of time (called as dwell time, or measurement time) to capture every single noise component [19]. The measured spectrum is therefore a linear combination of emissions caused by separate switching events [16].

These events are not dependent on each other, thus can be analyzed separately. The simulated radiated emission is the superposition of the individually simulated radiated emission profiles corresponding to the individual switching states.

In case of a simple DC-DC buck converter, two separate simulations shall be performed:

- Spectral excitation at the switching MOSFET with the corresponding spectrum envelope, while the diode is represented by its junction capacitance,
- Spectral excitation at the diode with the corresponding spectrum envelope, while the switching MOSFET is represented by its equivalent drain-source capacitance.

The result of these simulations are a set of AC voltages and currents. The last step of the proposed method is to sum the results of both simulations. This post-processing step gives the combined radiated emission profile of the high-side and low-side switching operation of the DC-DC converter.

V. RADIATED EMISSION MODELING

A. *Test setup*

According to the international standard CISPR25 [19], radiated emission tests shall be performed in a semi-anechoic chamber. In the frequency domain 100 kHz – 30 MHz the radiated emission is measured using a 1-meter-long monopole antenna, which is usually equipped with a built-in amplifier. The test setup is specified in the fourth edition of CISPR25. The test arrangement shall be put on an elevated metallic table, which galvanically connected to the outer shield of the chamber. Apart from the floor, every side of the chamber shall be covered with ferrite tiles and pyramid absorbers to minimize the chamber related effects on the measurement results. The absorption ratio of the walls shall be at least 6 dB in the 70 – 2500 MHz frequency range. Below 70 MHz, the absorption performance is not specified. The pyramidal absorbers are not suitable to be used in the sub-100 MHz range [5].Without any dissipative medium, the cavity resonances of the chamber would distort the electric field distribution leading to incorrect measurement results. Hence, ferrite tiles are used to dissipate electromagnetic energy, which effectively decreases the quality factor of the cavity resonances.

B. *Modeling test environment properties*

The radiated emission test setup consists of 3 different parts that needed to be modelled with exceptional care, which all have a major effect on the simulated radiated emission results:

- Test setup,
- Chamber wall,
- Antenna.

These parts affect the simulated radiated emission. In case just a qualitative simulation is required, some of these

effects are negligible, however a quantitative simulation requires the engineer to pay close attention to any - seemingly irrelevant – details of the system. Considering and integrating these effects into a simulation model is essential to get a proper model, that could be used as a virtual EMC testing environment.

1) Test setup modeling

The test setup described in CISPR25 allows the test engineer to prepare the test arrangement with room for minor deviations. As an example, the length of the harness between the tested device, and the line impedance stabilization network can be freely chosen in the range 1.7 – 2 m. While at first it seems negligible, this and many similar parameters of the setup can have a major effect on the measurement results. The most important parameters of the automotive radiated emission test setup and their effect on the electromagnetic environment inside the chamber are the following:

- Device location and orientation:
  - Common and differential mode noise
  - Capacitive coupling between the device and the antenna
- Harness model:
  - Common and differential mode noise
  - Test setup resonance frequency
- Line Impedance Stabilization Network:
  - Common and differential mode noise
  - Standing wave along harness

The accurate modelling of the test setup is an indispensable step, while creating a simulation setup to be used for quantitative investigations.

The common mode noise is one of the most important artifacts of the automotive EMC test setup due to the additional metallic table in close proximity to the harness and the device. The higher the measurement frequency, the higher the influence of the common mode radiation on the radiated emission test results.

The capacitive coupling between the device under test and the metallic table is the main coupling path of the radiated emission test setup below 100 MHz, since the measuring antenna is in the near field of the radiating source [8][9].

2) Chamber wall modelling

Apart from the floor, which – according to CISPR25 – shall be a metallic plane, the walls of the semi-anechoic chambers shall show higher than 6 dB absorption along the frequency range of 70 – 2500 MHz. The absorption is usually achieved by combining ferrite tiles and pyramidal absorbers as the wall of anechoic chambers. Since the effective frequency ranges for ferrite tiles and the absorber pyramids are not identical, the applicable chamber wall model depends on the frequency range in interest. Depending on the alloy used to manufacture the ferrite tiles, the effective range may start at 30 MHz could provide proper performance up to 1000 MHz [5], meanwhile pyramidal absorbers are usually designed to absorb electromagnetic power above a couple of 100 MHz (which is also depending on the absorber material and size). Apart from the absorption, the chamber wall also serves as a shield against external electromagnetic noises to ensure the quietness of the testing area. A typical layered anechoic-chamber wall is shown in Fig. 6. The modelling of each layer – considering, that the frequency range of interest is below 30 MHz – is as follows.

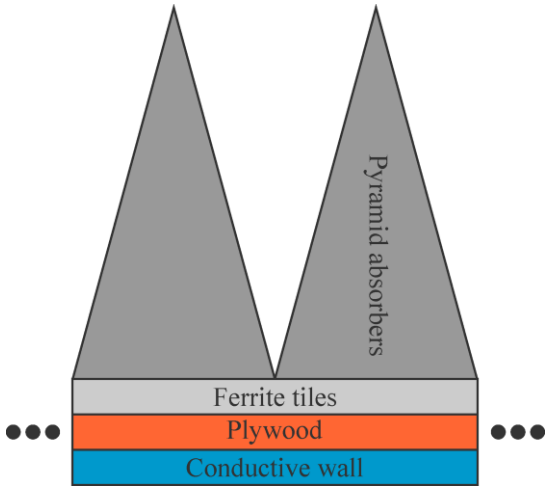

Fig. 4. Layered structure of the wall of an anechoic chamber.

a) Conductive wall

The lowest frequency of automotive radiates emission tests is 100 kHz. The wall of a shielded chamber is usually made of galvanized iron, or other good conductors. Depending on the conductivity, the skin depth [11] of the wall material is at most 1 mm. A wall constructed of metal sheets with a thickness of a couple of mm-s can be considered as infinitely thick, since the ratio of the electromagnetic power passing through the metallic wall is negligible. Therefore, it is permissible to consider the wall as a perfect electrical conductor (PEC), which can be easily applied as a boundary condition by ensuring, that the electric field is parallel to the external boundary of the simulation domain.

b) Ferrite tiles on plywood

Ferrite tiles are mounted on a thin layer of plywood to ensure the safety of the ferrite during assembly. Plywood can be easily taken into account by just setting the relative permittivity of this layer to 2.2. While it may seem to be exaggeration, a relative permittivity higher than one helps to concentrate the electric field near the ferrite tiles, thus improving the absorption indirectly.

The permeability characteristics of ferrites are complex, and frequency dependent. There are various techniques to model the frequency characteristics of such materials [20][21]. A widely used technique is the first order Debye-model, which can be expressed as

$$\mu_r(f) = \mu_\infty + \frac{\mu_s - \mu_\infty}{1 + \mathrm{j}f\tau}, \tag{3}$$

where $\mu_r(f)$ is the complex and frequency dependent permeability, μ_s and μ_∞ represent the real part of permeability at 0 and infinite frequency, while τ stands for the relaxation time. The above equation gives a macro model for the permeability, however, the assembly of ferrite

tiles in a semi-anechoic chamber cannot be performed perfectly, small gaps between ferrite tiles are inevitable. The effective permeability of a ferrite tile layer with gaps can be calculated according to the formula [22]

$$\mu_{r,eff}(f) = \frac{\mu_r(f)}{1 + \frac{\Delta}{l}(\mu_r(f) - \mu_{air})}, \quad (4)$$

which is widely used in magnetic circuitry theory. Here, l represents the width of the ferrite tile, while Δ is the dimension of air gap. Taking into account the air gap effects, the corrected model parameters corresponding to the ferrite tiles in the semi-anechoic chamber used for measurements are:

- $\mu_s = 1100$
- $\mu_\infty = 1$
- $\tau = 5\ ns$

The characteristics described by the parameters above can be observed in Fig. 5.

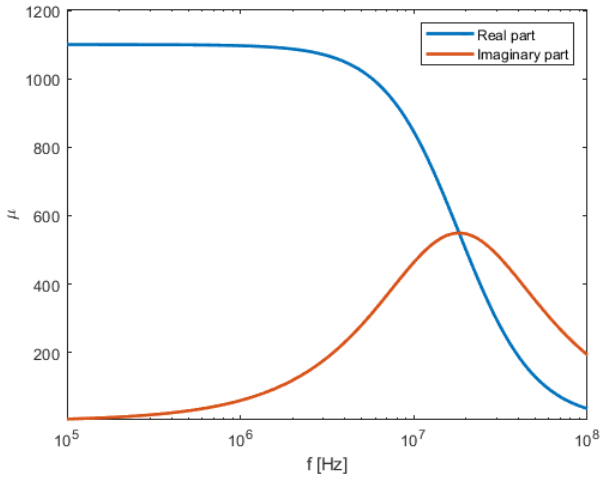

Fig. 5. Ferrite tile's permeability characteristics.

Ferrite tiles are attached to a thin layer of plywood, since the ferrite tiles are quite brittle, and may break during assembly. Depending on the manufacturing, the plywood layer has a relative permittivity around 2. The smallest wavelength in the monopole antenna range is way too large (10 m at 30 MHz) compared to the thickness of the plywood layer (16 mm in this case), therefore the plywood layer can be simply considered as air, since it won't affect the electromagnetic environment inside the chamber.

c) Pyramidal absorbers

The effective absorptive range of the commercially available pyramidal absorbers starts above 30 MHz [5]. This means, that the electromagnetic environment in the monopole range is not affected by the presence of the absorbers, therefore, these may be neglected from the simulation model, and can be considered as air. This is essential in decreasing the computational resources required for chamber simulations, since the usage hundreds of pyramidal shapes with complex permeability characteristics can be avoided.

d) Monopole antenna

According to CISPR 25, the monopole antenna to be used for EMC testing below 30 MHz shall have a length of 1 m, and shall be located at 1 m distance from the test setup, which is very small compared to the wavelength. Therefore, the antenna is electrically small, and is in the near field of the test setup. Under these circumstances, the monopole antenna is capacitively coupled to the test setup, radiation does not occur.

The commercially available monopole antennas have an integrated amplifier, which needs to be taken into account during simulation, since from AC point of view, it acts as a capacitance parallel to the monopole antenna.

C. Simulation workflow

The approach proposed in this paper has 3 main steps. These are:

- Excitation modelling
- 3D simulation model preparation
- Simulation and post-processing

The workflow that describes the procedure of the quasi-quantitative combined small-signal analysis can be seen in Fig. 6. The excitation spectrum may be prepared based on switching waveform measurement, circuit level simulation, or may be even analytically calculated by knowing the input and output voltages and the switching frequency according to (1) and (2). By applying numerical simulation on the 3D model, the *S*-parameter [23] representation of the whole 3D structure can be extracted. The circuitry, the antenna impedance, and the line impedance stabilization network is then attached to the *S*-parameter model, and small signal analysis is performed with the switching noise spectrum for the high-side and low-side switching component. The antenna voltage is then multiplied by the antenna factor to obtain the electric field at the antenna. The dwell-time for a radiated emission measurement is usually between 5 – 50 ms [19], which allows to capture the switching noise multiple times within a single measurement. This means that a measurement performed with a peak detector would show the absolute highest noise power detected during the dwell-time. Two emission spectrums are generated by exciting the high-side and low side switching component separately. The switching events are well separated in time (see in Fig. 2.), therefore the emission caused by the switching events cannot interfere with each other, thus the overall simulated emission shall be the maximum of both simulated electric fields.

To obtain the most accurate simulation results, it is essential to take special care for all the steps and models, since a minor mismatch between the real and simulated parameters might lead to unpredictable error in the simulation results. Despite the huge amount of careful modelling and obtainable model parameter, the quasi-quantitative combined small-signal analysis approach can be still considered as a simplification compared to the full transient simulation, meanwhile the time required for simulations are drastically decreased due to the fact, that AC analysis is performed instead of transient simulation.

The order of magnitude of the acceleration greatly depends on the simulated system. 3D simulation is necessary for both, which results in a frequency dependent *S*-parameter model of the simulation setup. For time-

harmonic simulation, only the relevant frequency components need to be simulated, while in case of transient analysis, the steady state shall be reached, and then the spectrum can be calculated by FFT. To give an idea on the magnitude of acceleration, in the frequency range under investigation, the 3D simulation of the whole test setup with a simplified PCB model took around 5 minutes with our hardware, A single transient analysis also took around 5 minutes, while the time-harmonic simulation provides almost immediate results. If the simulation engineer only performs 1-1 simulation run, around 2x acceleration can be achieved. If parametric analysis is performed, then the acceleration factor can be much higher.

Since the excitation signal is not dependent on the design parameters, any part of the DC-DC converter may be parametrically analysed, without the need to re-evaluate the excitation signals. By co-simulating the 3D model and the attached circuitry, the filter design and the layout optimization can be evaluated within the same optimization cycle.

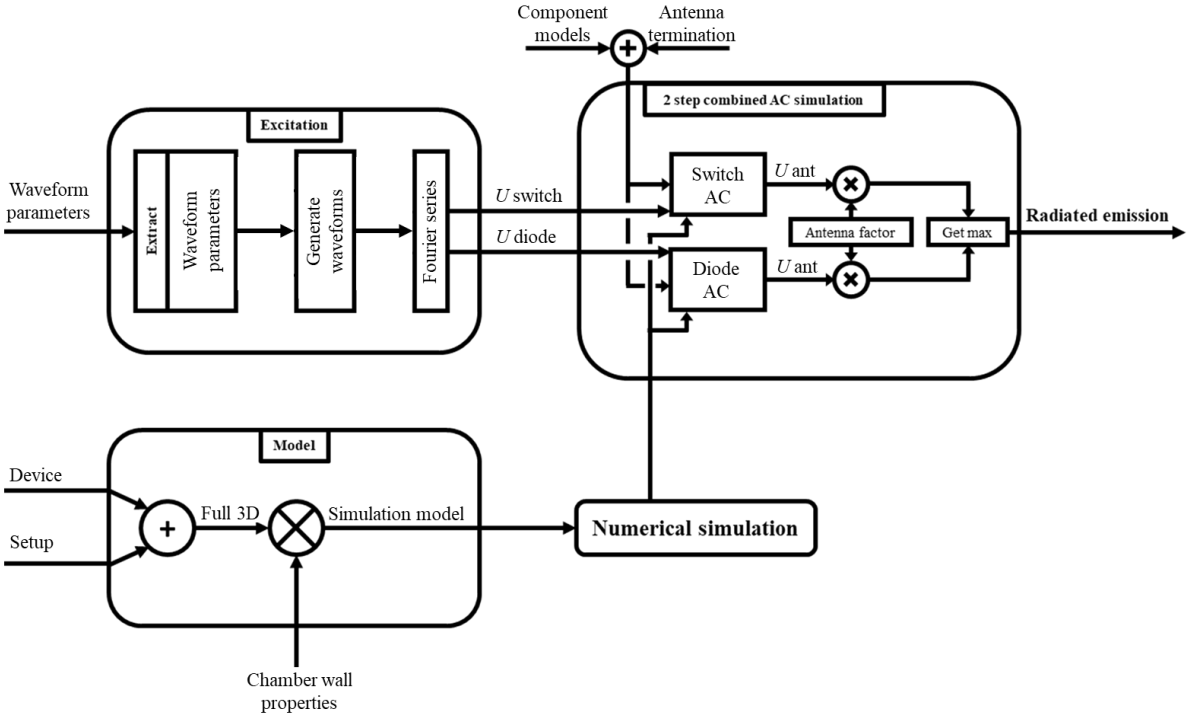

Fig. 6. Workflow of the proposed method.

VI. Results

To present the effectiveness of the proposed method, the evaluation board for Texas Instrument's TPS54560 switching IC [24] has been measured and simulated. The switching parameters were the following:

- Input voltage: 13 V
- Output voltage: 5 V
- Duty cycle: ~38 %
- Switching frequency 415 kHz

In order to have a clean comparison between measurement and simulation, the harmonics of the switching frequency have been extracted from the measured emission profile. Since the switching is the only noise source in the system, it is permissible to ignore the noise at frequencies not related to the switching frequency harmonics.

Simulations have been performed using Ansys HFSS [25] with the direct solver in frequency domain using finite element method [26].

The size of the simulated semi anechoic chamber in the model is:

- Width: 4300 mm
- Length: 5500 mm
- Height: 3500 mm

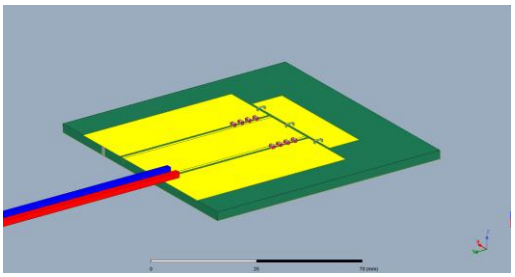

Fig. 7. Simplified model of the DC-DC buck converter.

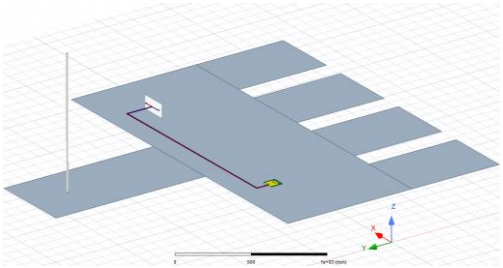

Fig. 8. Radiated emission test setup simulation model. Chamber wall hidden.

The comparison of measured and simulated emission characteristics can be observed in Fig. 8. The simulated results fit very well to the measured characteristics, the difference is mostly below 3dB, which is comparable to the usual measurement uncertainty for radiated emission measurements in semi-anechoic chambers. It can be observed that the difference between measured and simulated results is increased in the frequency range of 7 – 20 MHz. Since this frequency range is mostly affected by the ferrite tile's complex and nonlinear permeability characteristics (observe the graph in the above mentioned frequency range in Fig. 5.), it is highly probable, that the macro model for the ferrite tiles is not sufficiently accurate to properly capture the losses, since the gaps between the ferrite tiles can vary greatly.

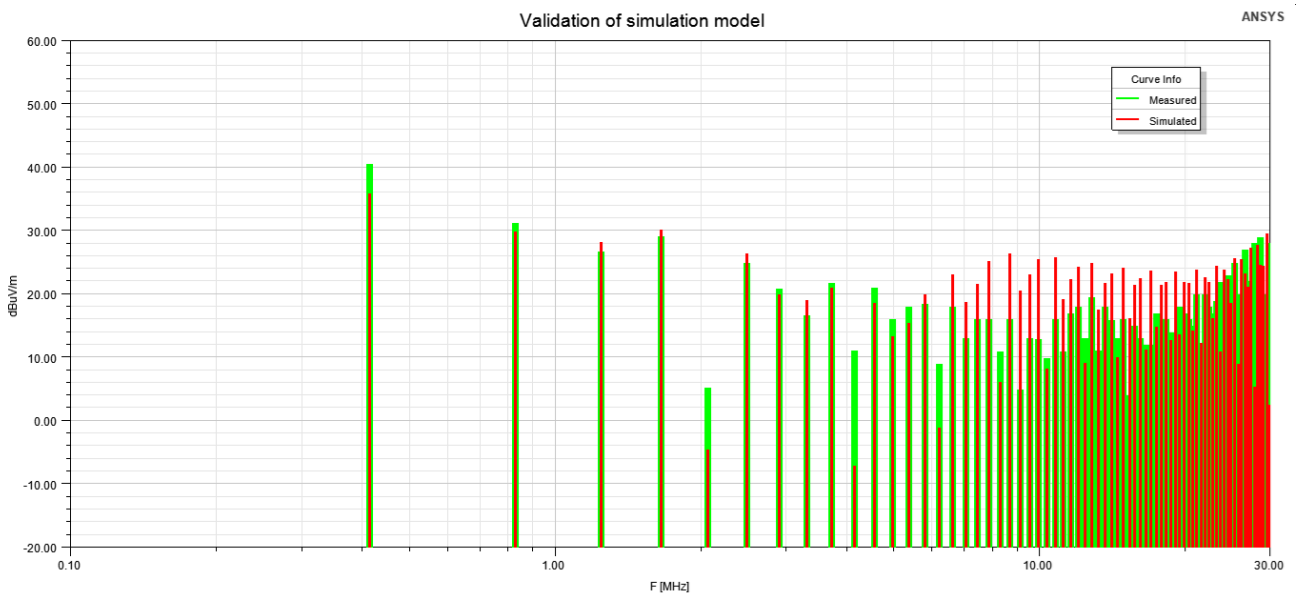

Fig. 9. Comparison of measured and simulated radiated emission.

VII. Conclusion

A quasi-quantitative small signal analysis approach has been presented to accurately simulate radiated emission characteristics caused by switching noise. Detailed explanation has been given for the presented workflow. The modelling steps has been shown, and the most crucial points has been emphasized. The efficiency of the proposed simulation technique has been presented through a comparative investigation on the radiated emission of the evaluation board for TPS54560 switching IC. The simulation result fits to the measured characteristics within the expected accuracy. The cause for the mismatch is addressed, further investigations will follow the paper to establish an even more accurate simulation technique.

The main advantage of the proposed approach compared to other methodologies is, that by exciting the system with the spectrum of the trapezoid signal, there is no need for time consuming transient analysis, enabling quick parametric investigations even on the 3D model, which is essential for electromagnetic compatibility engineers. Another aspect that makes the proposed method more attractive is the relatively simple workflow, which does not require pre-measurements and preparing complex SPICE models for the switching components.

References

[1] J. Hansen, C. Potratz, "Capacity extraction in physical equivalent networks", 2015 IEEE International Symposium on Electromagnetic Compatibility, pp. 491-496, 2015.

[2] T. H. Hubling, H.-W. Shim, "Model for estimating radiated emissions from a printed circuit boards with attached cables due to voltage-driven sources", IEEE transactions on Electromagnetic Compatibility, vol. 47, no. 4, pp. 899-907, 2005.

[3] P. Hillenbrand, M. Böttcher, S. Tenbohlen, J. Hansen, "Transient co-simulation of electromagnetic emission caused by a SiC traction inverter", 2017 International Symposium on Electromagnetic Compatibility – EMC EUROPE, pp. 1-6, 2017.

[4] S. Niedzwiedz, S. Frei, "Transient emission analysis of EV- and HEV-powertrains using simulation", IEEE International Symposium on Electromagnetic Compatibility, pp. 247-252, 2013.

[5] S. H. Raad, "Analysis and Design of Absorbers for Electromagnetic Compatibility Applications", In Recent Topics in Electromagnetic Compatibility, London: IntechOpen, 2021. DOI: 10.5772/intechopen.100543.

[6] M. K. Kazimierczuk, "Pulse-width modulated DC-DC power converters", Wiley, Dayton, Ohio, 2008.

[7] Tsai-Fu Wu, "The origin of converters", in 2013 1st International Future Energy Electronics Conference (IFEEC), Tainan, 2013, pp. 611-617.

[8] Richtek, Application Note 045, "Reducing EMI in buck converters", 2016.

[9] Murata, "EMI solution for DC/DC converter", 2016.

[10] E. Darie and E. Darie, "EMI Problems associated with DC-DC Converters", Proceedings of the 7th WSEAS International Conference on Power Systems, pp. 232-235, 2007.

[11] C. R. Paul, "Introduction to electromagnetic compatibility, 2nd Edition", Wiley, New York, 2006.

[12] G. Friedl, P. Prukner, M. Kuczmann, "Qualitative small-signal analysis of DC-DC buck converter's radiated emission", 12th IEEE International Conference on Cognitive Infocommunications, pp. 103-108, 2021.

[13] Texas Instruments, Application Note SLUA831A, "Minimizing switching ringing at TPS53355 and TPS53353 family devices", 2017.

[14] Z. Chen, Y. Yao, D. Boroyevich, K. Ngo, P. Mattavelli, "Exploration of switching loop snubber for parasitic ringing suppression", Proc. IEEE Energy Convers. Congr. Expo., pp. 1605-1612, 2014.

[15] S. W. Ng, S. C.Wong and Y. S. Lee, "Small signal simulation of switching converters", IEEE Transactions on Circuits and Systems, Vol. 46, No. 6, pp 731-739, Jun. 1999.

[16] P. Hillenbrand et. al., “Frequency-domain EMI-simulation and resonance analysis of a DCDC-converter”, EMC Europe, Wroclaw, Poland, 2016, pp. 176-181.

[17] C. Rostamzadeh et. al., “Investigation of electromagnetic field coupling from DC-DC buck converters to automobile AM/FM antennas”, IEEE International Symposium on Electromagnetic Compatibility, Ottawa, pp. 364-369, 2016.

[18] M. Bocher, “Introduction to the theory of Fourier’s series”, Annals of Mathematics, vol. 7, no. 3, pp. 81-152, 1906.

[19] “CISPR 25: Limits and Methods of Measurement of Radio Disturbance Characteristics for Protection of Receivers Used on Board Vehicles ,3rd ed.”, Geneva, Switzerland IEC, 2008.

[20] X. Liu, F. Grassi, G. Spadacini, S. A. Pignari, F. Trotti, N. Mora, W. Hirschi, “Behavioral modeling of complex magnetic permeability with high-order Debye model and equivalent circuits”, IEEE Transactions on Electromagnetic Compatibility, vol. 63, no. 3, pp. 730-738, 2021.

[21] I. Zivkovic, A. Murk, “Free-space transmission method for the characterization of dielectric and magnetic materials at microwave frequencies”, Microwave Materials Characterization, London, United Kingdom: IntechOpen, 2012.

[22] K. Liu, “Analysis of the effect of ferrite tile gap on EMC chamber having ferrite absorber walls”, Proceedings of Symposium on Electromagnetic Compatibility, pp. 156-161, 1996.

[23] D. M. Pozar, „Microwave Engineering - 4th edition”, Wiley, 2012.

[24] Texas Instruments, User’s Guide SLVU863, “Evaluation module for the TPS54560 step-down converter”, 2013.

[25] Ansys HFSS, https://www.ansys.com/products/electronics/ansys-hfss.

[26] M. Kuczman, A. Iványi, “Finite element method in magnetics”, Academic Press, Budapest, 2008.

[27] Z. Kubík, S. Jiří, “Electromagnetic interference from DC/DC converter of photovoltaic system”. 2019 International Conference on Applied Electronics (AE). IEEE, 2019.

[28] Z. Ma, Y. Lai, Y. Yang, Q. Huang, S. Wang, “Review of Radiated EMI Modeling and Mitigation Techniques in Power Electronics Systems”, In 2023 IEEE Applied Power Electronics Conference and Exposition (APEC), pp. 1776-1783, 2023.

[29] Y. Lai, Y. Yang, Z. Ma, Q. Huang, S. Wang, Z. Luo, “Development of Simulation Prediction Techniques for Low Frequency Emissions”, In 2023 IEEE Applied Power Electronics Conference and Exposition (APEC), pp. 2690-2696, 2023.